Carbohydrate Polymers 102 (2014) 38–46

Contents lists available at ScienceDirect

Carbohydrate Polymers

journal homepage: www.elsevier.com/locate/carbpol

Pyridine derivative covalently bonded on chitosan pendant chains for textile dye removal

Cintia S. Oliveira, Claudio Airoldi*

Institute of Chemistry, University of Campinas, UNICAMP, P.O. Box 6154, 13084-971 Campinas, SP, Brazil

ARTICLE INFO

Article history:
Received 20 May 2013
Received in revised form 17 October 2013
Accepted 24 October 2013
Available online 1 November 2013

Keywords:
Chitosan
Pyridine derivative
Sorption
Dye
Non-linear regression

ABSTRACT

Chitosan was chemically modified through a sequence of four reactions with immobilized 2-aminomethylpyridine at the final stage, after prior protection of amino group with benzaldehyde. The characterized biopolymers containing free amino and hydroxyl active centers on the biopolymeric structure and pyridinic nitrogen on pendant chains showed combined hydrophobic properties that can potentially favor interactions. Reactive Yellow GR and Blue RN dyes gave the maximum sorption capacities of 2.13 and 1.61 mmol g^{-1}, which were performed as functions of contact time, concentration and dye structure. However, biopolymer/dye interactions are governed by effective hydrogen bond and van der Waals forces for such structural adjustments. The data obtained from the concentration isotherm were applied to non-linear regressions of the Langmuir, the Freundlich and the Sips models, with the best fit to the latter model. The kinetic data was fitted to non-linear regression of pseudo-second-order, indicating that the sorption phenomena are most likely to be controlled by chemisorption process.

1. Introduction

Colored organic effluents originating from the textile, paper, plastic, leather, food, and mineral processing industries constitute undesirable wastewater that aggregate pigments or dyes, which can cause serious water pollution problems (Messina & Schulz, 2006). Small amounts of colored wastes such as dye not only are esthetically displeasing, but also hinder light penetration, to disturb the biological processes in water bodies (Chao et al., 2005; Messina & Schulz, 2006).

Various physical, chemical and biological methods have been extensively explored for dye-containing wastewater management, which include chemical coagulation, flocculation, chemical oxidation, photochemical degradation, membrane filtration, including aerobic and anaerobic biological degradations (Dizge, Aydiner, Demirbas, Kobya, & Kara, 2008; Won et al., 2006). However, dye-contained wastewater is very difficult to amend, since the dyes are recalcitrant organic molecules, resistant to aerobic digestion, stable to light, heat and oxidizing agents and chemical oxidation results in aromatic ring cleavage, generating more toxic chemical sludge or by-products (Won et al., 2006).

Amongst numerous techniques for dye removal, sorption is a choice procedure, which sorbent should have low-cost, be highly efficient, simple, easy to recovery/reuse and be insensitive to toxic substance properties (Alkan, Demirbas, & Dogan, 2007; Wu, 2007). It has also a specific advantage if it removes the dye molecule completely, unlike other techniques applied for this purpose that can destroy only the dye chromophore part, leaving harmful residual moieties in the effluent (Wu, 2007).

Nowadays, attention has been focused on inexpensive and efficient materials, capable of pollutant removal from contaminated aqueous solution to replace the most used activated carbon (Moscofian, Pires, Vieira, & Airoldi, 2012; Tang, Zhang, Guo, & Zhou, 2007). Based on a variety of sorbents, natural polymers such as alginate, pectin, cellulose, chitin and chitosan have attracted attention not only due to their excellent sorption capability, but also some properties associated with environment-friendly behavior such as renewable, biocompatible, biodegradable and nontoxic nature have been considered (Iqbal, Saeed, & Zafar, 2009; Wang & Wang, 2008).

From these biopolymers chitosan, extracted from crustacean shrimp, crab and lobster shells, exoskeleton of insects and the cell walls of some fungi has also been used as sorbent (Juang, Wu, & Tseng, 2002; Lopes, Sousa, & Airoldi, 2009). Chitosan the linear and typically 20% acetylated (1 → 4)-2-amino-2-deoxy-β-D-glucan, is isolated from marine chitin (Muzzarelli, 1977; Muzzarelli et al., 2012). From the structural point of view, chitin and chitosan are very similar, containing reactive hydroxyl and amino groups, being chitosan less crystalline than chitin, which presumably makes it more accessible to reagents, such as aldehydes and ketones in a typical Schiff reaction, in particular, with a series of benzaldehydes (Muzzarellli, 1988; Ravi Kumar, Muzzarelli, Muzzarelli, Sashiwa, & Domb, 2004).

* Corresponding author. Tel.: +55 19 35213055; fax: +55 19 35213023.
E-mail address: airoldi@iqm.unicamp.br (C. Airoldi).

0144-8617/$ – see front matter © 2013 Published by Elsevier Ltd.
http://dx.doi.org/10.1016/j.carbpol.2013.10.075

Chitosan and chemical derivatives have been extensively investigated due to the non-toxicity, hydrophilicity, high biocompatibility and biodegradability properties, in addition to attractive physical and mechanical domains. The low cost and relatively easy preparative methods, these polymers give many academic and also practical uses in medicine, agriculture, food technology and cosmetic applications (Machado, Lopes, Sousa, & Airoldi, 2009), presented also in various forms as powder, paste, film, fiber etc. (Agnihotri, Mallikarjuna, & Aminabhavi, 2004).

The present investigation deals with chemically modified chitosan, using previous protection of the amino group with benzaldehyde. This derivative favors the reaction of the hydroxyl group on carbon 6 with epichlorohydrin molecule, to permit inclusion of the epoxide group, which is easily opened through reagents containing a free electron pair as 2-aminomethylpyridine. After complete reaction, benzaldehyde was eliminated in acidic condition and the available basic active sites have the ability to remove pollutants, as evaluated for Reactive Yellow GR (RY) and Reactive Blue RN (RB) dyes in aqueous solutions.

2. Materials and methods

2.1. Materials

Powered chitosan with 82% degree of deacetylation was obtained by extraction from crab shells and supplied by Primex Ingredients A.S. The reagents benzaldehyde (Aldrich), methyl and ethyl alcohols (Synth), 2-aminomethylpyridine (Aldrich), epichlorohydrin (Synth), hydrochloric acid (Synth), sodium hydroxide (Gold). Reactive Yellow GR and Reactive Blue RN dyes were received as a gift from DyStar Ltda, Suzano, SP, Brazil and were used without prior purification in aqueous solutions.

2.2. Syntheses of chitosan derivatives

2.2.1. Chitosan-benzaldehyde

Chitosan amino groups were initially protected with benzaldehyde to favor the reaction of the more reactive hydroxyl group on carbon 6. For this synthesis 5.0 g of powdered chitosan were suspended in 60.0 cm^3 of methanol, then 20.0 cm^3 of benzaldehyde were slowly added, and the suspension was stirred for 24 h at room temperature (Tang et al., 2007; Yi, Wang, & Ye, 2006). The obtained solid was isolated, washed several times with methanol and dried at 333 K during 8 h, to yield the biomaterial named (1 → 4)-2-amino-2-deoxy-2-N-benzidine-β-D-glucan (BZL).

2.2.2. Chitosan-benzaldehyde with epichlorohydrin

For this synthesis 4.0 g of the preceding biomaterial were suspended in 120.0 cm^3 of a 1.0×10^{-3} mol dm^{-3} sodium hydroxide solution at 323 K, and then 6.0 cm^3 of epichlorohydrin were slowly added. The mixture was stirred for 6 h and the solid obtained was filtered and washed with water and acetone and dried at 333 K during 8 h, to produce the biomaterial (1 → 4)-2-amino-2-deoxy-2-N-benzidine-6-2-(chloromethyl)oxirane-β-D-glucan (EAC).

2.2.3. Chitosan-benzaldehyde with 2-aminomethylpyridine

An amount of 3.0 g of the preceding biomaterial was suspended in 90.0 cm^3 of 1.0×10^{-3} mol dm^{-3} sodium hydroxide at 333 K, and then 3.0 cm^3 of 2-aminomethylpyridine was slowly added. The mixture was stirred, filtered, washed and dried as before, to yield the biopolymer (1 → 4)-2-amino-2-deoxy-2-N-benzidine-6-[O-butyl-4-2aminepyridyl)-β-D-glucan (CTA).

2.2.4. Benzaldehyde removing

This process was performed in acidic medium, using an ethanolic solution containing 0.24 mol dm^{-3} hydrochloric acid. To this solution, 2.0 g of powdered CTA biopolymer was suspended in 60.0 cm^3 of solution and stirred at room temperature for 24 h. The solid obtained (1 → 4)-2-amino-2-deoxy-2-6-[O-butyl-4-2aminepyridyl)-β-D-glucan (CTN), was filtered and washed with water and dried at 333 K for 8 h, as schematically showed in Fig. 1.

2.3. Characterization

Percentages of carbon and nitrogen for chitosan and derivatives were determined through elemental analyses on a Perkin Elmer model PE 2400 elemental analyzer. Infrared spectra of the samples in KBr pellets were obtained by accumulating 32 scans on a Bomem spectrophotometer, MB-series, model B 100, in the 4000–400 cm^{-1} range, with 4 cm^{-1} of resolution. Nuclear magnetic resonance spectra for the carbon nucleus in the solid state were obtained on a Bruker–Avance II^+ 300 spectrometer at room temperature, using the CP-MAS technique, with contact time 4 ms, relaxation time 3 s and frequency of 75.47 MHz. The thermogravimetric curves in an argon atmosphere were obtained on a TA instrument, coupled to a model 2050 thermobalance, using a heating rate of 0.167 K s^{-1}, varying from room temperature to 1073 K. X-ray diffraction patterns were performed on Shimadzu diffractometer, model XRD-7000 (40 kV, 30 mA), in the $2\theta = 2.5–50^\circ$ range using nickel-filtered Cu-Kα radiation, with a wavelength of 0.154 nm. For the determination of zero point charge (pH_{PZC}) for the biopolymers, samples of 15.0 mg were suspended in 15.0 cm^3 of aqueous 0.010 mol dm^{-3} sodium chloride, having pH varying from 3 to 10, adjusted with sodium hydroxide or hydrochloric acid solutions. The suspensions were shaken for 24 h in an orbital bath at 298 ± 1 K. The final pH of the supernatant was then measured using a Metter Toledo pHmeter (Santos, Vilar, & Boaventura, 2008; Vieira et al., 2010; Vieira, Cestari, Carvalho, Oliveira, & Chagas, 2012).

2.4. Sorption experiments

Solutions of RY and RB anionic dyes having concentrations ranging from 1.6×10^{-4} to 3.2×10^{-3} and 1.1×10^{-3} to 3.8×10^{-3} mol dm^{-3}, respectively, were used for all sorption processes. For each experiment, a series of polyethylene flasks, containing about 10 mg of CTN biopolymer was kept in contact with 10.0 cm^3 of dye solutions, using the established concentration ranges. The suspensions were placed in a thermostatic bath at 298 ± 1 K and orbitally stirred for a period of 24 h. Subsequently, in order to determine the concentration of dye in equilibrium, the solid was separated by centrifugation using a Hettich Zentrifugen model Rotina 38 instrument at 4000 rpm for 5 min. The aliquots of supernatant were analyzed by spectrophotometer (UV–vis) at wavelengths of 416 and 592 nm for RY, RB dyes, respectively. The amount of sorbed dye in mmol g^{-1} were calculated by Eq. (1), where N_f is the number of moles of dye sorbed onto the biopolymer, n_i and n_s are the initial number of moles of dye and number of moles in the supernatant at equilibrium number and m is the mass of the sorbent used in each sorption process (Sousa, Silva Filho, & Airoldi, 2009).

$$Nf = \frac{n_i - n_s}{m} \quad (1)$$

2.5. Kinetic studies

The kinetic experiments for RB and RY dyes with CTN were performed with solutions of concentrations of 2.7×10^{-3} and 3.0×10^{-3} mol dm^{-3} at 298 ± 1 K, respectively. In each experiment, about 10 mg of biopolymers were orbitally stirred with 10.0 cm^3 of dye solution. At predetermined times aliquots were taken from the supernatant and analyzed by ultraviolet–visible (UV–vis) absorption spectroscopy. Identically, for all other intermediates BZL, EAC

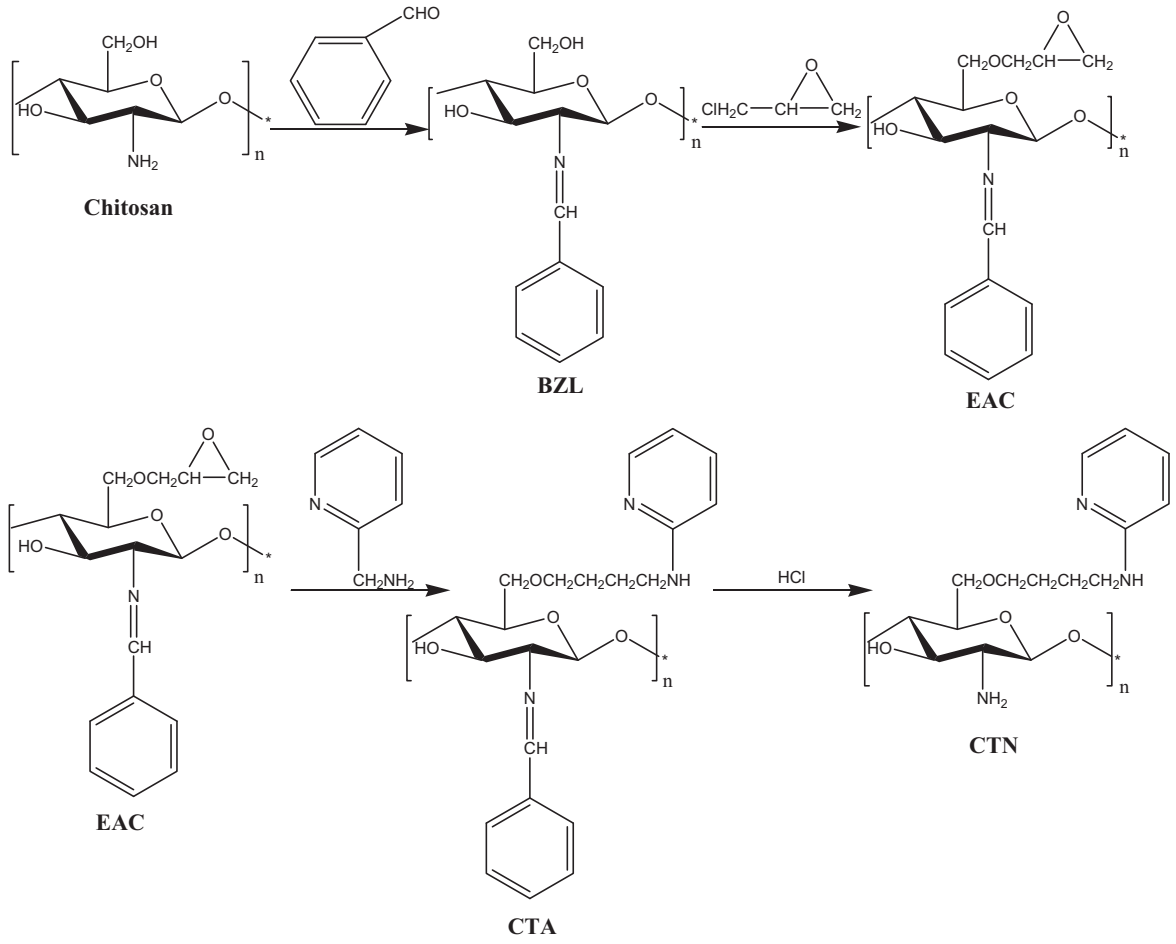

Fig. 1. Reaction scheme to obtain chitosan pyridine derivatives.

and CTA the same procedure was applied with 3.0×10^{-3} mol dm^{-3} RY, considering only one determination in the saturated CTN condition, with the objective to compare the degree of sorption. Again, the amount of dye sorbed in the experiments was calculated by Eq. (1).

3. Results and discussion

3.1. Elemental analyses

Percentages of carbon and nitrogen for the chitosans obtained, the values of each element also expressed in terms of their number of moles per gram of each biopolymer and carbon/nitrogen molar ratio (C/N) are listed in Table 1. After chitosan chemically modified with benzaldehyde, there is an increase in this relationship, due to the incorporation of the carbon containing moiety proceeding from benzaldehyde, into the original polymeric structure. The other biopolymers exhibited a decrease in C/N values, when compared to the BZL ratio, but generally with increases in comparison to chitosan. For CTA biopolymer an increase of nitrogen relative to BZL is observed, due to the incorporation of the pyridine derivative. The decrease in C/N ratio for CTN is a clear confirmation of the removal of the benzaldehyde. As a general procedure, the calculated percentage values were obtained from the molar mass of each monomeric unit, after incorporating any moiety as pendant chains and for chitosan this value was 161 g mol^{-1}. With the exception of the EAC biopolymer a good agreement was observed for experimental and calculated C/N ratios, as these values corroborated with the sequence of proposed reactions. Based on these values the degree of substitution (Malkondu, Kocak, & Yilmaz, 2009) was also calculated through Eq. (2), as listed in Table 1.

$$C_1/N_1(1-X) + (C_2/N_2)X = (C_3/N_3)0.82 \quad (2)$$

where C_1/N_1 is the calculated value for nonsubstituted chitosan, C_2/N_2 for chitosan derivative and C_3/N_3 the experimental elemental analysis for each sample. The calculated amount of substitution degree X for each biopolymer was based on the precursor biopolymer with 0.82% of deacetylation. As observed, EAC biopolymer has the lowest degree of substitution and CTA presented the highest value (Ravi Kumar et al., 2004).

3.2. Infrared spectroscopy

The infrared spectra of chitosan and all derivatives are shown in Fig. 2. The spectrum of chitosan provides an intense and broad band at 3436 cm^{-1} attributed to OH stretching vibration frequency, which band overlaps the amino stretching vibration in the same region (Lopes et al., 2009; Sousa et al., 2009). The band at 1324 cm^{-1} is related to aliphatic CH bending vibrations and those at 2910 cm^{-1} correspond to the stretching vibrations of the same groups. Characteristics bands at 1648 and 1381 cm^{-1} are attributed to C=O stretching and C—H deformation bands of acetamide groups, respectively, presented in chitosan due to incomplete chitin deacetylation. The band at 1596 cm^{-1} is attributed to NH bending associated to amide II (Lopes et al., 2009; Sousa et al., 2009). The bands in the 1200–800 cm^{-1} region are assigned to the pyranosidic ring, such as β-glucosidic C—O—C bonds, as well as the C—O bond of primary and secondary alcohols (Machado et al., 2009).

Table 1
Percentages of carbon (C) and nitrogen (N) experimental (exp) and calculated (calc), the respective number of moles, molar ratio (C/N) and degree of substitution of all biopolymers (Biop).

Biop	C_{exp} (%)	N_{exp} (%)	C_{exp} (mmol g^{-1})	N_{exp} (mmol g^{-1})	C_{calc} (%)	N_{calc} (%)	C/N_{calc}	C/N_{exp}	DS
CHT	42.45	7.77	35.38	5.55	44.72	8.69	6.00	6.37	–
BZL	58.06	4.99	48.38	3.56	62.65	5.62	13.02	13.59	0.72
EAC	52.71	5.68	43.92	4.06	62.95	4.59	15.99	10.81	0.26
CTA	49.98	6.32	41.65	4.51	64.08	10.19	7.34	9.23	1.24
CTN	35.49	6.48	29.58	4.63	55.55	12.96	5.00	6.39	0.82

The spectra of the biopolymers BZL, EAC and CTA present additional characteristic bands in comparison to chitosan, related to angular deformation of the carbon–hydrogen bonds of the aromatic ring (Silverstein, Bassler, & Morril, 2000; Yang & Li, 2002; Yi et al., 2006), in the 692–750 cm^{-1} interval, indicating the presence of benzaldehyde in these biopolymers. These bands were not observed in the CTN spectrum that feature is very relevant to confirming the removal of benzaldehyde from the preceding biopolymer. However, for the CTN spectrum a new band that appeared at 1530 cm^{-1} corresponds to the vibration of the pyridine ring, in agreement with the insertion of pyridine derivative into the chitosan structure (Silverstein et al., 2000). The supposed band related to nitrogen–hydrogen bond in the 3500–3300 cm^{-1} interval was not observed, since it is the same region that corresponds to the vibration of free OH and NH_2 group in the original chitosan (Silverstein et al., 2000; Sousa et al., 2009). The band associated with C—H bond stretching located at 2910 cm^{-1} in the spectra of chitosan, appears at 2923 cm^{-1} in the CTN spectrum. The band at 2871 and 2891 cm^{-1} for chitosan and in the CTN spectra correspond to carbon–hydrogen stretching vibration bond of CH_2 group.

To investigate possible dye sorption on CTN, the infrared spectra of centrifuged samples obtained in the maximum sorption condition for biopolymer/dye combinations were identically dried as the precursor biopolymer, and the isolated dyes were also obtained. It is observed, in principle, that the main characteristic bands associated with the biopolymer are maintained for these two sets of CTN–dye combinations. However, additional bands associated with the dyes, with more intensity in the free dye, mainly in the 750 cm^{-1} region, clearly demonstrate that the biopolymer is bonded by both dyes. For both biopolymers the presence of the bands related to dyes are confirmed and for the CTN-RB spectrum showed characteristic bands of the pure dye as visualized at 621, 680, 764, 1278 cm^{-1}, as well as bands of the precursor biopolymer at 897, 1024, 1080 cm^{-1}. The same behavior is also observed for the other dye, in agreement with similar sorption processes. Therefore, it was not possible to obtain information on the sorption mechanism, since the spectra of biopolymer and biopolymer containing dye were very similar. It is worth noting that dye/biopolymer interactions confirm the adjustment of the dye structure on biopolymer chains involving possible hydrogen bond formations that were reinforced by van der Waals interactions, due to the hydrophobicity of both dye and biopolymer species.

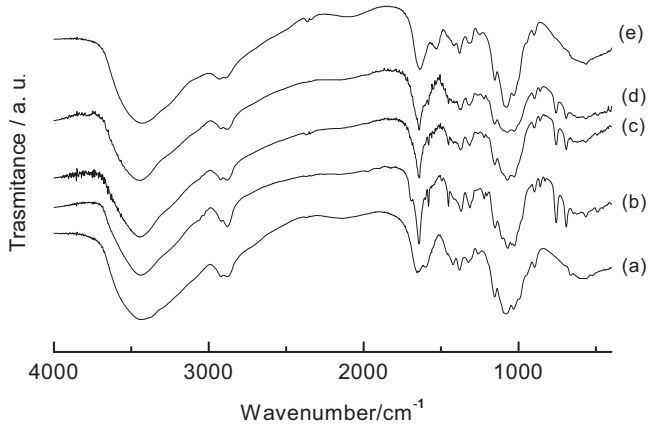

Fig. 2. Infrared spectra of chitosan (a), BZL (b), EAC (c), CTA (d) and CTN (e).

3.3. X-ray diffraction

The X-ray diffractograms for chitosan present two broad peaks at 11° and 20°, indicating low crystallinity of the polymers (Lopes et al., 2009; Machado et al., 2009; Sousa et al., 2009). For the derivatives BZL, EAC and CTA, the presence of a new peak at 6.5° and the decrease in the intensity of the second peak, indicates the modification in the polymeric structure, possibly due to the incorporation of functional groups in the polymer backbone, which promote the disruption of hydrogen bonds in the original chains, as shown in Fig. 3. As expected, the CTN biopolymer has broad peaks at 12 and 23°, with a small change in intensity, indicated that this biomaterial is less organized as compared to the original polymeric structure. In general, the chitosan derivatives have less polymeric chain organization related to the precursor polymer (Machado et al., 2009; Sousa et al., 2009). Thus, the crystallinity of chitosan reflected the intra and intermolecular hydrogen bonds that are present in the polymer in order to maintain stability (Machado et al., 2009; Sousa et al., 2009). However, after incorporation of new functional groups in the moiety chains, changes in the orientation of the original polymeric chains due to the expected hydrogen bonds disruption, are reflect in the crystallinity behavior.

3.4. NMR spectroscopy

The magnetic resonance spectra for the carbon nucleus in solid state for all biopolymers are shown in Fig. 4. The chitosan spectrum presents chemical shifts at 102, 54, 79 and 57 ppm, related to the C1, C2, C4 and C6 carbons, respectively, as well as a signal at 75 ppm related to the C3, C5 carbons, present in its structure. The signals

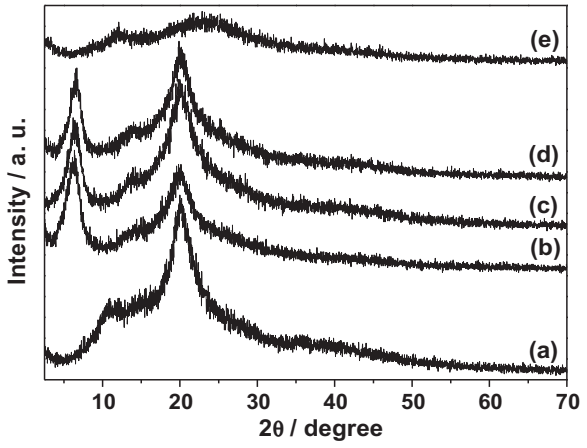

Fig. 3. X-ray diffraction patterns of chitosan (a), BZL (b), EAC (c), CTA (d) and CTN (e).

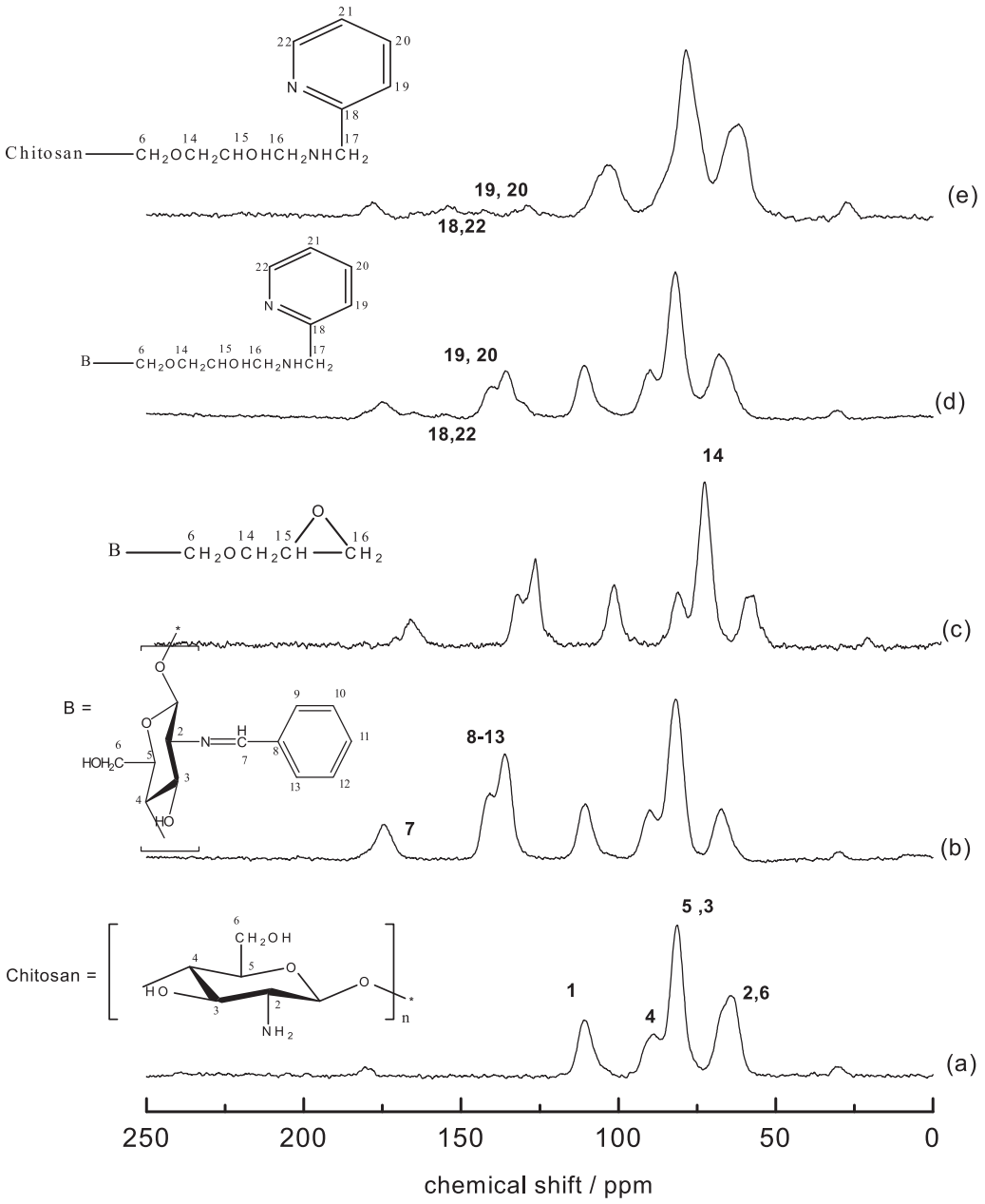

Fig. 4. ^{13}C NMR spectra in the solid state of chitosan (a), BZL (b), EAC (c), CTA (d) and CTN (e) biopolymers.

at 21 and 170 ppm are assigned to methyl and carbonyl groups in the chitosan structure due to incomplete deacetylation of chitin (Monteiro & Airoldi, 1999; Sousa et al., 2009). For the BZL, EAC and CTA spectra the characteristic peak at 129 ppm is attributed to the aromatic carbon of benzaldehyde (Yang & Li, 2002; Yi et al., 2006). This peak is absent in the CTN spectrum, as expected, that also confirms the removal of benzaldehyde from the preceding structure. Comparing the chitosan spectrum with the derivatives, it is observed that the signals related to C2 and C6 carbons are superimposed and appear as a single signal. Moreover, in the CTN spectrum the signal for C4 is not present, while a broad signal was observed for the C1 carbon. Such differences in the profiles of the spectra confirm the modification of chitosan.

3.5. Thermogravimetry

The thermogravimetric profiles for chitosan and chemically modified biopolymers are very similar and the stages of decompositions are better represented by the derivative forms. An illustration of this behavior for chitosan and CTN biopolymers are shown in Fig. 5 and from these curves the decomposition stages can be obtained. For example, chitosan presented a mass loss in two stages, in the 323–353 and 539–594 K intervals, corresponding to 9.4 and 60.7% of mass losses, attributed to water and organic moiety elimination during polymer heating (Machado et al., 2009; Sousa et al., 2009).

With the exception of the BZL derivative all other biopolymers presented two stages of mass losses that are very close to the same events of pristine chitosan decomposition stages. For BZL the mass losses steps at 312–335, 378–427 and 545–588 K ranges were observed, corresponding to 5.3, 3.1 and 54.9%, respectively. The EAC, CTA biopolymers have two stages of mass losses at temperatures slightly lower and similar to chitosan.

The EAC biopolymer presented stages of decomposition in the 319–348 and 492–597 K intervals, with 7.7 and 49.4% of mass losses, while CTA biopolymer gave mass losses of 324–349 and

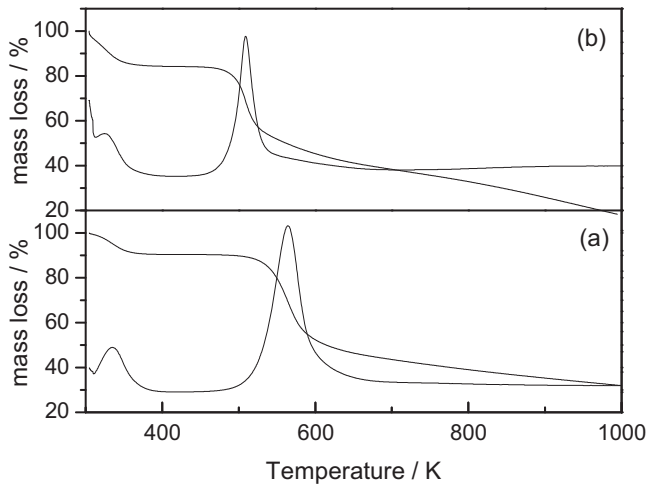

Fig. 5. Thermogravimetric and their derivative curves for chitosan (a) and CTN (b) biopolymers.

528–588 K ranges that correspond to 9.8 and 49.0%, respectively. Based on these results it is observed that the chemically modified biopolymers that showed lower decomposition temperatures, are thermally less stable than chitosan. Furthermore, CTN biopolymer has a significant mass loss at lower temperatures than chitosan and also presents lower thermal stability than the other biopolymers. The temperature ranges of decomposition for CTN were 308–348 K and 495–529 K intervals, with mass losses of 14.5 and 47.0%, respectively.

3.6. Zero point charge

The variation of the pH values before and after addition of the biopolymer ΔpH versus initial pH for CTN biopolymer plot gave the zero charge point value of 5.20 for the biopolymer. The surface charge is dependent on the pH of the solution, if it has a value lower than PZC ($pH < pH_{PZC}$) the surface of the material will be positively charged and thus can sorb anions. On the other hand, if the pH value is higher than PZC ($pH > pH_{PZC}$), then the surface will be negatively charged and cationic species can be sorbed (Vieira et al., 2012). The pH of the dye solutions used is near to pH 6.0, indicating that the material is slightly negatively charged.

The expected substrate/dye interactive effect is directly dependent on the available active centers on both structural arrangements. The dyes chosen for the present investigation are originally formulated as sodium salts, which in aqueous solutions present in anionic form with a net negative charge due to the dissociation of the sodium sulfonate groups (SO_3^-) (Al-Degs, El-Barghouthi, El-Sheikh, & Walker, 2008). Thus, such structures enable simultaneous interactions related to chemical bonding, ion-exchange, hydrogen bond, hydrophobic attraction, van der Waals force, physical sorption, aggregation mechanism, dye–dye interactions etc.

The focused substrate derived from chitosan, whose original biopolymer behaved as an acceptor agent during dye sorption, using not only the most active amine center, but also hydroxyl groups, especially in the monomeric C3 position, to lead to the intermolecular interactions to form stable chitosan–dye systems (Crini & Badot, 2008). However, for biopolymer/dye interaction a portion related to hydrophobic effects must be considered, beyond the most pronounced hydrogen bond formations.

The synthesized chitosan derivatives with increases in available active centers can interact with dyes that are sensible to the acidity of the medium. The same behavior is valid for the dyes that can be protonated to favor electrostatic interactions with the substrate as the pH increased. Since the sorption experiments were performed in aqueous solution, where the biomaterial is negatively charged, it is believed that van der Waals forces and hydrogen bonding have significant influence on the sorption process (Crini & Badot, 2008). In these conditions, the charged biopolymer surface is negative, which hinders sorption by electrostatic force of repulsion between the negatively charged dye molecule and sorbent. Then, there is possibility of hydrogen bond formation between components of dyes as nitrogen, sulfur and oxygen centers, as well as benzene ring and $-CH_2OH$ groups of the chitosan biopolymer (Chatterjee, Chatterjee, Chaterjee, & Guha, 2007), but the electrostatic interaction is not favored under these conditions. In addition, the hydrophobic interactive effect also has participation in these kinds of interactions, as both structures are adjusted in a complete overlap (Moscofian et al., 2012).

3.7. Sorption

Sorption isotherms ideally describe how a given sorbate interacts with the sorbent to give a critical behavior in optimizing features associated with the chosen process of a desired sorbent (Wang, Xiang, Cheng, & Li, 2010). This process is thus essential to correlate the equilibrium data by either theoretical or empirical models for designing a perfect operating sorption system for industrial effluents (Chatterjee et al., 2007). An accurate mathematical description of equilibrium sorption capacity is indispensable for reliable prediction to achieve the goal related to sorption parameters and quantitative comparison of sorption behavior for different sorbent systems or for varied experimental conditions (Gimbert, Morin-Crini, Renault, Badot, & Crini, 2008). For this purpose, the equilibrium data can usually be explored based on the classical Langmuir, Freundlich and Sips models.

Currently, the Langmuir model has been widely used to characterize interactive processes that happen at the solid/liquid interface. This sorption model predicts the existence of monolayer coverage by the sorbate at the outer surface of the sorbent. So, a basic assumption is that sorption takes place at specific homogeneous sites within the sorbent, where all sorption sites are identical and energetically equivalent. It is then assumed that once a sorbate occupies a site, no further sorption can take place at that site (Gimbert et al., 2008; Wong, Szeto, Cheung, & Mckay, 2004). Moreover, the isotherm equation further assumes that no interactions exist between molecules at adjacent sites (Vieira, Cestari, Santos, & Dias, 2005), which sorption process can be mathematically described by Eq. (3):

$$Nf = \frac{N_s b C_s}{1 + bCs} \tag{3}$$

where N_f is the amount sorbed (mmol g^{-1}), C_s the sorbate concentration (mmol dm^{-3}) in solution at the equilibrium, b the Langmuir constant (dm^3 $mmol^{-1}$) and N_s the maximum sorption capacity for monolayer formation on the sorbent surface (mmol g^{-1}) (Wang et al., 2010).

The Freundlich isotherm describes heterogeneous systems and reversible sorption processes. This isotherm is an empirical equation used for the description of multilayer sorption with interaction between sorbed molecules when bonded to the surface. Thus, the model predicts that the sorbate concentrations on the sorbent surface will increase with increase in sorbate concentration in the solution to reach surface saturation (Chatterjee et al., 2007; Gimbert et al., 2008) and the representative model is described by equation:

$$Nf = Kf(Cs)^{1/n} \tag{4}$$

where C_s (mmol dm^{-3}) is the liquid-phase sorbate concentration at equilibrium, N_f (mmol g^{-1}) the amount sorbed at equilibrium,

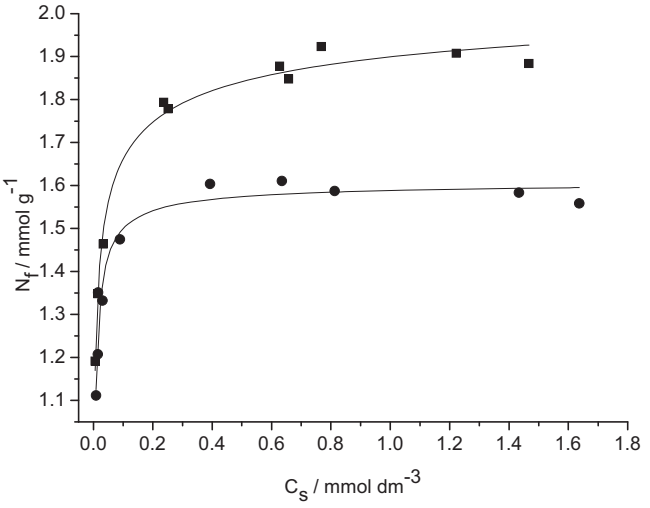

Fig. 6. Isotherm of time for RY (■) and RB (●) dye sorptions on biopolymer CTN.

K_f the Freundlich constant related to sorption capacity and $1/n$ the heterogeneity factor (Anirudhan & Senan, 2011; Wang et al., 2010).

The Sips isotherm is a combination between the Langmuir and the Freundlich expressions deduced for predicting heterogeneous sorption systems and takes advantage of the limitation of the rising sorbate concentration associated with the Freundlich isotherm model (Foo & Hameed, 2010). Therefore, at low sorbate concentrations it effectively reduces to the Freundlich isotherm, while at high concentrations it predicts a monolayer sorption capacity that characterizes the Langmuir isotherm (Anirudhan & Senan, 2011; Foo & Hameed, 2010). Then, the Sips model is given by equation:

$$Nf = \frac{N_s b(C_s)^{1/n}}{1 + b(C_s)^{1/n}} \quad (5)$$

where N_s is the maximum sorption capacity (mmol g^{-1}), b the association constant related to sorption capacity and $1/n$ the heterogeneity factor (Anirudhan & Senan, 2011; Foo & Hameed, 2010). The resulting values for $1/n$ lower than unit are in agreement for a heterogeneous system, while values closer to or even equal to one indicate a material with relatively homogenous binding sites. In this case the Sips model is reduced to the Langmuir equation (Anirudhan & Senan, 2011).

The data obtained for the isotherm of concentration for the dyes are shown in Fig. 6 were fitted to three specific models through non-linear regression, using Origin 8.0 software and the resulting parameters are listed in Table 2. The applicabilities of these isotherm equations are evaluated by the coefficient of correlation, R^2, and nonlinear chi-square test, χ^2. The application of χ^2 is used to evaluate the best fit of the isotherm to experimental data and the smaller the better is the final fit (Karadag, 2007).

Table 2
Summary of data obtained from non-linear regression models for the interaction of dyes with the biopolymer CTN.

Model	Parameter	RY	RB
Langmuir	N_s (mmol g^{-1})	1.851	1.582
	b (dm^3 $mmol^{-1}$)	242.957	263.651
	$\chi^2/10^{-3}$	10.160	2.540
	R^2	0.8557	0.9224
Freundlich	K_f (mmol g^{-1})	1.920	1.600
	N	12.330	18.037
	$\chi^2/10^{-3}$	3.740	6.140
	R^2	0.9470	0.8127
Sips	N_s (mmol g^{-1})	2.132	1.611
	b (dm^3 $mmol^{-1}$)	8.170	69.067
	N	2.747	1.407
	$\chi^2/10^{-3}$	0.981	2.310
	R^2	0.9861	0.9295

The experimental data for RY and RB dye sorptions with CTN biopolymer showed good fits for the Freundlich and the Langmuir models. The choice of this final synthesized biopolymer for the sequence of reactions is clearly justified. For example, considering the maximum sorption capacity of 1.85 mmol g^{-1} for RY dye obtained from the Langmuir model, as shown in Table 2, is much higher than the equivalent value for BZL, EAC and CTA biomaterials that gave 0.60; 0.33 and 0.50 mmol g^{-1}, respectively. A good fit for CTN reflected in the highest R^2 values (close to 1) and lowest χ^2 values obtained. On the other hand, the Sips model yielded a better fit to the experimental data than the Freundlich and Langmuir models. Based on this application for the Sips model it is suggested that the biomaterial exhibits a heterogeneous surface.

Dye uptake by the chemically modified biopolymer gave the order: RY > RB with sorption capacities of 2.132 and 1.611 mmol g^{-1}, respectively. These results demonstrated that the dye structures strongly influence the sorption processes. For example, RY dye is relatively planar or linear and presents a short carbon chain, so its molecular structure makes the diffusion inside the biopolymer easy and also favors the hydrophobic interaction with the solid. On the contrary, RB dye presents an intramolecular interaction between SO_3^- and NH_2 groups, both positioned in the benzene ring. Thus, the first group seems to cause a decrease of the effectiveness in the electrostatic interaction. Moreover, this more branched structural disposition could hinder diffusion and affect the hydrophobic interactions (Moscofian et al., 2012).

3.8. Kinetic studies

Sorption kinetic data were investigated taking into account the Lagergreen pseudo-first-order and pseudo-second-order models. The first-order rate expression is based on the capacity of the solids, as really occurs with this system, but in some conditions involving substrate/sorbent interactions they do not fit well over the entire extent of the processes and it is generally adaptable over the initial 20–30 min of sorption (Aksu & Dönmez, 2003; Hasan, Ahmad, & Hameed, 2008). Identically, a pseudo-second-order equation is also based on the sorption capacity of the solid phase, assuming that the rate limiting step may be chemical sorption involving sharing or exchange of electrons between anionic dyes and biosorbent (Aksu & Dönmez, 2003; Hasan et al., 2008). The pseudo-first-order and pseudo-second-order models (Anirudhan & Senan, 2011; Karadag, 2007) can be described by Eqs. (6) and (7):

$$Nf(t) = Nf(eq)(1 - e^{-(k_1 t)}) \quad (6)$$

$$Nf(t) = \frac{k_2 (Nf(eq))^2 t}{1 + k_2 Nf(eq) t} \quad (7)$$

where k_1 is the rate constant of pseudo-first-order (min^{-1}), $N_{f(t)}$ and $N_{f(eq)}$ the amounts of dye sorbed at time t and at equilibrium (mmol g^{-1}), k_2 the pseudo-second-order rate constant of sorption (g $mmol^{-1}$ min^{-1}).

The isotherms for both dyes on the biopolymer CTN are shown in Fig. 7. As observed, the profiles for both curves indicate that the equilibrium condition was reached in less than 900 min. Based on this behavior the sorption mechanism for these data were fitted to kinetic pseudo-first order and pseudo-second-order models. The $N_{f(eq)}$, k_1 and k_2 values were determined by a non-linear regression procedure using Origin 8.0 software and the results obtained are listed in Table 3.

The theoretical $N_{f(eq)}$ values estimated from the pseudo-second-order kinetic model gave almost similar values compared to the

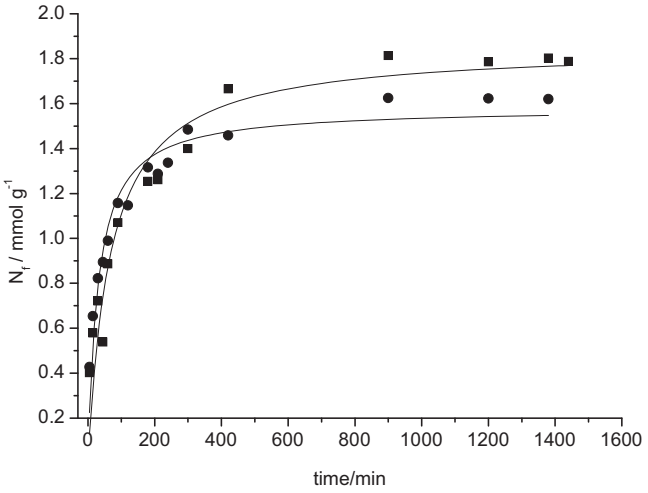

Fig. 7. Influence of concentration of RY (■) and RB (●) dye sorptions on CTN biopolymer.

experimental data. R^2 values for pseudo-second-order model are very close to unity and χ^2 values are lower, suggesting that the kinetics of dye sorption can be described by the pseudo-second-order model and this process is most likely to be controlled by chemisorption, which may involve sharing or exchange of electrons between dye anions and sorbent (Aksu & Dönmez, 2003; Karadag, 2007).

In general, the mechanism for dye removal by sorption on an sorbent material may be assumed to involve the following four steps: (i) migration of dye from the bulk of the solution to the surface of the sorbent, (ii) diffusion of dye through the boundary layer to the surface of the adsorbent, (iii) transport of the dye from the surface to within the pores of the particle and (iv) sorption of dye at an active site on the surface of material via ion-exchange, complexation and/or chelation. The data obtained indicate that the present sorption process may involve the four described steps, where the interaction with the biopolymer occurred not only on the surface of the biomaterial, but also, as expected, inside the pores. However, the relevant pyridine nitrogen atom attached to the pendant chain clearly participated in this sorption process, which organic function in chitosan derivatives effectively can act as mediated gene delivery system (Sajomsang et al., 2013).

The effectiveness of dye removal related to sorption capacities for RY and RB with molar masses of 620 and 626 g mol^{-1} leads to 1321 and 1009 mg of the respective dyes per gram of biopolymer. These values are only comparable to phyllosilicate with 1343 and 1286 mg g^{-1} for RY and RB (Moscofian et al., 2012). However, other sorbents as silica and mesoporous carbon gave 351 (Moscofian, Pires, Vieira, & Airoldi, 2013) and 176 mg g^{-1} (Macedo et al., 2006) for RY and 388 mg g^{-1} for RB (Moscofian et al., 2013) with the last sorbent. As observed, the chitosan derivative acts as efficient sorbent in a relatively simple, inexpensive and alternative method to other techniques that are generally not effective or generate undesirable by-products. In this context, other investigations demonstrated that chitosan presents higher capacity to remove reactive dyes over other sorbents, including activated carbon and other sorbents of low cost (Crini & Badot, 2008). In spite of reduced studies with these dyes, the present investigation contributes to the understanding of the high utility of the chitosan derivative to dye removal from an ecosystem.

Table 3
Kinetic parameters obtained from non-linear regression models for dye/biopolymer CTN interactions.

Model	Parameter	RY	RB
Pseudo-first-order	$N_{f(eq)}$ (mmol g^{-1})	1.708	1.448
	k_1 (min^{-1})/10^{-2}	0.932	2.272
	χ^2/10^{-2}	4.029	2.625
	R^2	0.8408	0.8068
Pseudo-second-order	$N_{f(eq)}$ (mmol g^{-1})	1.862	1.581
	k_2 (mmol g^{-1} min^{-1})/10^{-2}	0.735	2.093
	χ^2/10^{-2}	2.234	0.912
	R^2	0.9118	0.9329

4. Conclusions

The synthetic procedure of a series of reactions to chemical modify chitosan showed that in the final stage the pendant chains contain 2-aminomethylpyridine groups, as confirmed by the characterization results, which biopolymer effectively removes anionic dyes from aqueous solutions. Among the dyes investigated, the biomaterial showed a higher ability to remove Reactive Yellow, suggesting that the shorter and relatively planar carbon chain favors the diffusion of the dye inside the biopolymer. It is proposed that dye/biopolymer interactions should occur mainly through van der Waals forces and hydrogen bond formation and also involve basic dye atoms such as nitrogen, oxygen and sulfur. The experimental data of equilibrium for the dye sorptions fitted better to the Sips model, indicating that the biomaterials have heterogeneous sites. The kinetic data better fitted to pseudo-second-order indicating that chemisorption is the rate controlling step, which may involve sharing or exchanging of electrons between anionic dye and sorbent. Therefore, the high content of dye removal per gram of biopolymer expresses the effectiveness of this sorbent as a good candidate to clean up an ecosystem.

References

Agnihotri, S. A., Mallikarjuna, N. N., & Aminabhavi, T. M. (2004). Recent advances on chitosan-based micro- and nanoparticles in drug delivery. *Journal of Controlled Release*, *100*, 5–28.
Aksu, Z., & Dönmez, G. A. (2003). A comparative study on the biosorption characteristics of some yeast for Remazol Blue reactive dye. *Chemosphere*, *50*, 1075–1083.
Al-Degs, Y. S., El-Barghouthi, M. I., El-Sheikh, A. H., & Walker, G. M. (2008). Effect of solution pH, ionic strength, and temperature on adsorption behavior of reactive dyes on activated carbon. *Dyes and Pigments*, *77*, 16–23.
Alkan, M., Demirbas, O., & Dogan, M. (2007). Adsorption kinetics and thermodynamics of an anionic dye onto sepiolite. *Microporous and Mesoporous Materials*, *101*, 388–396.
Anirudhan, T. S., & Senan, P. (2011). Adsorption characteristics of cytochrome C onto cationic Langmuir monolayers of sulfonated poly(glycidylmethacrylate)-grafted cellulose: Mass transfer analysis, isotherm modeling and thermodynamics. *Chemical Engineering Journal*, *168*, 678–690.
Chao, L., Zhaoyang, L., Aimin, L., Wei, L., Zhenmao, J., Jinlong, C., et al. (2005). Adsorption of reactive dyes onto polymeric adsorbents: Effect of pore structure and surface chemistry group of adsorbent on adsorptive properties. *Separation and Purification Technology*, *44*, 91–96.
Chatterjee, S., Chatterjee, S., Chaterjee, B. P., & Guha, A. K. (2007). Adsorptive removal of Congo Red, a carcinogenic textile dye by chitosan hydrobeads: Binding mechanism, equilibrium and kinetics. *Colloids and Surfaces A*, *299*, 146–152.
Crini, G., & Badot, P. M. (2008). Application of chitosan, a natural aminopolysaccharide, for dye removal from aqueous solutions by adsorption processes using batch studies: A review of recent literature. *Progress in Polymer Science*, *33*, 399–447.
Dizge, N., Aydiner, C., Demirbas, E., Kobya, M., & Kara, S. (2008). Adsorption of reactive dyes from aqueous solutions by fly ash: Kinetic and equilibrium studies. *Journal of Hazardous Materials*, *150*, 737–746.
Foo, K. Y., & Hameed, B. H. (2010). Insights into the modeling of adsorption isotherm systems. *Chemical Engineering Journal*, *156*, 2–10.
Gimbert, F., Morin-Crini, N., Renault, F., Badot, P-M., & Crini, G. (2008). Adsorption isotherm models for dye removal by cationized starch-based material in a single component system: Error analysis. *Journal of Hazardous Materials*, *157*, 34–46.
Hasan, M., Ahmad, A. L., & Hameed, B. H. (2008). Adsorption of reactive dye onto cross-linked chitosan/oil palm ash composite beads. *Chemical Engineering Journal*, *136*, 164–172.
Iqbal, M., Saeed, A., & Zafar, S. I. (2009). FTIR spectrophotometry, kinetics and adsorption isotherms modeling, ion exchange and EDX analysis for understanding the mechanism of Cd^{2+} and Pb^{2+} removal by mango peel waste. *Journal of Hazardous Materials*, *164*, 161–171.

Juang, R., Wu, F., & Tseng, R. (2002). Use of chemically modified chitosan beads for sorption and enzyme immobilization. *Advances in Environmental Research*, *6*(171), 177.

Karadag, D. (2007). Modeling the mechanism, equilibrium and kinetics for the adsorption of Acid Orange 8 onto surfactant-modified clinoptilolite: The application of nonlinear regression analysis. *Dyes and Pigments*, *74*, 659–664.

Lopes, E. C. N., Sousa, K. S., & Airoldi, C. (2009). Chitosan–cyanuric chloride intermediary as a source to incorporate molecules – Thermodynamic data of copper/biopolymer interactions. *Thermochimica Acta*, *483*, 21–28.

Macedo, J. S., Costa Júnior, N. B., Almeida, L. E., Vieira, E. F. S., Cestari, A. R., Gimenez, I. F., et al. (2006). Kinetic and calorimetric study of the adsorption of dyes on mesoporous activated carbon prepared from coconut coir dust. *Journal of Colloid and Interface Science*, *298*, 515–522.

Machado, M. O., Lopes, E. C. N., Sousa, K. S., & Airoldi, C. (2009). The effectiveness of the protected amino group on crosslinked chitosans for copper removal and the thermodynamics of interaction at the solid/liquid interface. *Carbohydrate Polymer*, *77*, 760–766.

Malkondu, S., Kocak, A., & Yilmaz, M. (2009). Immobilization of two azacrown ethers on chitosan: evaluation of selective extraction ability toward Cu(II) and Ni(II). *Journal of Macromolecular Science Part A: Pure and Applied Chemistry*, *46*, 745.

Messina, P. V., & Schulz, P. C. J. (2006). Adsorption of reactive dyes on titania–silica mesoporous materials. *Journal of Colloid and Interface Science*, *299*, 305–320.

Monteiro, O. A C., Jr., & Airoldi, C. (1999). Some studies of crosslinking chitosan–glutaraldehyde interaction in a homogeneous system. *International Journal of Biological Macromolecules*, *26*, 119–128.

Moscofian, A. S. O., Pires, C. T. G. V. M. T., Vieira, A. P., & Airoldi, C. (2012). Organofunctionalized magnesium phyllosilicates as mono- or bifunctitonal entities for industrial dyes removal. *RSC Advances*, *2*, 3502–3511.

Moscofian, A. S. O., Pires, C. T. G. V. M. T., Vieira, A. P., & Airoldi, C. (2013). Removal of reactive dyes using organofunctionalized mesoporous sílicas. *Journal of Porous Materials*, *20*, 1179–1188.

Muzzarelli, R. A. A., Boudrant, J., Meyer, D., Manno, N., DeMarchis, M., & Paoletti, M. G. (2012). A tribute to Henri Braconnot, precursor of the carbohydrate polymers science, on the chitin bicentennial. *Carbohydrate Polymers*, *87*, 995–1012.

Muzzarelli, R. A. A. (1977). *Chitin*. Oxford: Pergamon Press.

Muzzarellli, R. A. A. (1988). Carboxymethylated chitins and chitosans. *Carbohydrate Polymers*, *8*, 1–21.

Ravi Kumar, M. N. V., Muzzarelli, R. A. A., Muzzarelli, C., Sashiwa, H., & Domb, A. J. (2004). Chitosan chemistry and pharmaceutical perspectives. *Chemical Reviews*, *104*, 6017–6084.

Sajomsang, W., Gonil, P., Ruktanonchai, U. R., Petchsangsai, M., Opanasopit, P., & Puttipipatkhachorn, S. (2013). Effects of molecular weight and pyridinium moiety on water-soluble chitosan derivatives for mediated gene delivery. *Carbohydrate Polymers*, *91*, 508–517.

Santos, S. C. R., Vilar, V. J. P., & Boaventura, R. A. R. (2008). Waste metal hydroxide sludge as adsorbent for a reactive dye. *Journal of Hazardous Materials*, *153*, 999–1008.

Silverstein, R. M., Bassler, G. C., & Morril, T. C. (2000). *Spectrometric identification of organic compounds* (6th ed.). New York: John Wiley & Sons.

Sousa, K. S., Silva Filho, E. C., & Airoldi, C. (2009). Ethylenesulfide as agent for incorporation into the biopolymer chitosan in a solvent-free reaction for use in cation removal. *Carbohydrate Research*, *344*, 1716–1723.

Tang, X., Zhang, S. S., Guo, C., & Zhou, A. (2007). Adsorption of Pb^{2+} on chitosan cross-linked with triethylene-tetramine. *Chemical Engineering Journal*, *30*, 955–961.

Vieira, A. P., Santana, S. A. A., Bezerra, C. W. B., Silva, H. A. S., Melo, J. C. P., Silva Filho, E. C., et al. (2010). Copper sorption from aqueous solutions and sugar cane spirits by chemically modified babassu coconut (*Orbignya speciosa*) mesocarp. *Chemical Engineering Journal*, *161*, 99–105.

Vieira, E. F. S., Cestari, A. R., Carvalho, W. A., Oliveira, C. S., & Chagas, R. A. (2012). The use of freshwater fish scale of the species Leporinus elongates as adsorbent for anionic dyes. *Journal of Thermal Analysis and Calorimetry*, *109*, 1407–1412.

Vieira, E. F., Cestari, A. R., Santos, E. B., & Dias, F. S. (2005). Interaction of Ag(I), Hg(II), and Cu(II) with 1,2-ethanedithiol immobilized on chitosan: Thermochemical data from isothermal calorimetry. *Journal of Colloid and Interface Science*, *289*, 42–47.

Wang, L., & Wang, A. (2008). Adsorption properties of congo red from aqueous solution onto N,O-carboxymethyl-chitosan. *Bioresource Technology*, *99*, 1403–1408.

Wang, Z., Xiang, B., Cheng, R., & Li, Y. (2010). Behaviors and mechanism of acid dyes sorption onto diethylenetriamine-modified native and enzymatic hydrolysis starch. *Journal of Hazardous Materials*, *183*, 224–232.

Won, S. W., Wu, G., Ma, H., Liu, Q., Yan, Y., Cui, L., et al. (2006). Adsorption performance and mechanism in binding of Reactive Red 4 by coke waste. *Journal of Hazardous Materials B*, *138*, 370–377.

Wong, Y. C., Szeto, Y. S., Cheung, W. H., & Mckay, G. (2004). Adsorption of acid dyes on chitosan-equilibrium isotherm analyses. *Process Biochemistry*, *39*, 693–702.

Wu, C.-H. (2007). Adsorption of reactive dye onto carbon nanotubes: Equilibrium, kinetics and thermodynamics. *Journal of Hazardous Materials*, *144*, 93–100.

Yang, Z., & Li, J. (2002). Preparation and characterization of dihydroxyl mesocyclic diamine derivative of chitosan. *Journal of Applied Polymer Science*, *86*, 2677–2681.

Yi, Y., Wang, Y., & Ye, F. (2006). Synthesis and properties of diethylene triamine derivative of chitosan. *Colloids and Surfaces A*, *277*, 69–74.